

3D weak lensing

Alan Heavens^{*}

Institute for Astronomy, University of Edinburgh, Royal Observatory, Blackford Hill, Edinburgh, EH9 3HJ, UK

26 October 2018

ABSTRACT

I propose an analysis method, based on spin-spherical harmonics and spherical Bessel functions, for large-scale weak lensing surveys which have source distance information through photometric redshifts. I show that the distance information can significantly reduce statistical errors on cosmological parameters; in particular, 3D lensing analysis offers excellent prospects for constraining the equation of state of the vacuum energy which dominates the energy density of the Universe. I show that the ratio of pressure to energy density could be determined to an accuracy of $\sim 1\%$ or better. Having distance information also offers significant advantages in the control of systematic effects such as the intrinsic alignment of galaxies. The case for obtaining photometric redshifts is therefore compelling. A signal-to-noise eigenmode analysis of the modes shows that the modes with highest signal-to-noise correspond quite closely to ignoring the redshift information, but there is significant extra information from a few radial modes. These modes are generally long-wavelength, suggesting that useful information can be gleaned even if the photometric redshifts are relatively inaccurate.

Key words: cosmology: observations - gravitational lensing - large scale structure, galaxies: formation

1 INTRODUCTION

As a direct probe of the mass distribution, gravitational lensing is an excellent tool for cosmological parameter estimation, complementing microwave background studies. Many of the cosmological parameters have been determined well from the microwave background, most recently and most accurately by the WMAP satellite (Spergel et al. 2003). There are some parameters which are difficult to constrain from the microwave background alone, the most significant example being the equation of state parameter ($w = p/\rho c^2$) of the vacuum energy. An accurate determination of w and its time-dependence is a major goal in the post-WMAP era, as it can put constraints on the nature of the vacuum energy. The direct mass dependence also offers advantages over studies of large-scale structure, which have to make assumptions about, or deduce, the relationship between galaxy and mass distributions on large scales (Verde L. et al. 2002). One of the most useful manifestations of gravitational lensing by intervening matter is the alignment of nearby images on the sky. Detection of dark matter on large scales through such ‘cosmic shear’ measurements has recently been shown to be feasible, and cosmological constraints from the first detections have now been made (e.g. Bacon, Refregier & Ellis 2000; Van Waerbeke et al. 2000; Brown et al. 2002a). To

date, the cosmic shear analyses have concentrated on using essentially only two-dimensional shear information; in surveys where (photometric) redshifts of the sources are known, they are used to determine the redshift distribution only, and are not used individually. Recently, though, 3D information has begun to be employed, mostly through what I would describe as $2\frac{1}{2}$ D analysis: the sources are divided into slices at different distances, based on their photometric redshifts, and a 2D analysis is done on each slice. This can be valuable in detecting the presence of clusters of galaxies (Wittman et al. 2001; Wittman et al. 2002; Taylor et al. 2003). At a statistical level, Hu (1999) has shown that there is some extra information on cosmological parameters which can be gained by dividing the sample this way. The extra information depends on the parameter under consideration: for the amplitude of the matter power spectrum, there are significant gains when the source population is split into two, but little is gained by further, fine subdivisions. For w , the gains are much larger, as the constraints from 2D lensing are weak. Finally, Taylor (2001) has shown how the lensing equations can be inverted to deduce the gravitational potential directly, and this offers exciting possibilities of reconstruction of the 3D mass density field from shear and convergence data (Bacon & Taylor 2002). Hu & Keeton (2002) have shown how this inversion can be done by matrix methods for discrete shear data in cells.

The purpose of this paper is to demonstrate how the full 3D information about the shear can be used. In particular,

^{*} afh@roe.ac.uk

I investigate how source photometric redshift information can be used in a statistical analysis to determine the mass power spectrum and the equation of state of the vacuum energy. In particular, we are interested in how much extra information on cosmological parameters can be gleaned from a 3D shear map, to see whether the reduction in statistical errors justifies the extra observing time required to obtain photometric redshifts for the sources.

Reducing statistical errors is, of course, not the only reason for wishing to have photometric redshifts; weak shear studies are beset by a number of systematic errors, and these may eventually dominate the error budget as surveys improve in scope and quality. The most obvious of these is the redshift distribution of the sources - ignorance of the precise distribution is already a source of significant error in current surveys (see e.g. Brown et al. 2002b). At a different level, the analysis of cosmic shear usually makes the assumption that the source galaxy ellipticities are uncorrelated, and this may not be true in detail, due to tidal effects during the galaxy formation process (Heavens, Refregier & Heymans 2000; Croft & Metzler 2000; Crittenden et al. 2001; Catelan, Kamionkowski & Blandford 2001; Mackey, White & Kamionkowski 2002; Jing 2002). The level of this effect is not well known, but it is thought to be large enough to be an important source of systematic error in low-redshift lensing surveys (Brown et al. 2002b; Heymans & Heavens 2003). By its nature, tidal effects are important for galaxies which are close together in three dimensions, so photometric redshifts can be used to remove or downweight nearby galaxy pairs in shear correlation estimates, for example Heymans & Heavens (2003), King & Schneider (2002). These studies show that the systematic effects of intrinsic alignments can be essentially completely removed, at the expense of an increase in shot noise. Other physical effects which could affect weak lensing studies can also be removed this way, for example the effects of source clustering if one uses number counts as a measure of magnification (Broadhurst, Taylor & Peacock 1995). Furthermore, with many (typically 5) images of galaxies available from a photometric redshift lensing survey, there is scope for better shape measurement, independent lensing studies and so on.

We see that there is a powerful case for obtaining photometric redshifts for lensing surveys on the basis of removing systematic errors. Having obtained distance information for the sources, it seems sensible to use it in the statistical analysis, as it must reduce the error bars on the parameters which one wants to estimate. In this paper, I propose a method, based on spherical Bessel functions and spin-spherical harmonics, for analysing such surveys.

I find that the 3D information can reduce the error on the amplitude of the matter power spectrum by a factor ~ 2 , which broadly speaking compensates for the extra time taken to obtain photometric redshifts. The error on the vacuum equation of state is encouraging: with 3D information w could be determined to an accuracy of $< 1\%$. These results assume that other cosmological parameters are known accurately, most plausibly from microwave background studies.

The paper is arranged as follows. Section 2 describes the method, section 3 discusses the expected errors, section 4 performs a signal-to-noise analysis of the modes, which turns out to be very informative, and section 5 presents the conclusions.

2 METHOD

2.1 Spherical coordinates and spherical Bessel functions

Spherical coordinates are natural for the description of fields on the full sky, but there are reasons for using them even if the sky coverage is relatively small. The survey specification is normally a combination of sky coverage (specified in terms of angular coordinates θ, φ), and depth (related to r). In addition, photometric errors introduce errors in r , and the lensing potential is related to the Newtonian potential by a radial integral. Having said this, the spherical harmonic expansion becomes cumbersome at high ℓ , and at some point a Fourier description on the flat sky becomes an attractive approximation to make. We choose to expand radially in spherical Bessel functions, as these (when combined with spherical harmonics) are eigenfunctions of the Laplace operator, which leads to a very simple relationship between the coefficients of the gravitational potential and those of the overdensity field, since these are related by Poisson's equation.

2.2 Transformation of scalar and shear fields

The spherical harmonic transform of a scalar field $f(\mathbf{r})$ is defined by

$$f_{\ell m}(k) \equiv \sqrt{\frac{2}{\pi}} \int d^3\mathbf{r} f(\mathbf{r}) j_{\ell}(kr) Y_{\ell}^{m*}(\Omega) \quad (1)$$

where $j_{\ell}(z)$ is a spherical Bessel function, Y a spherical harmonic, k is a wavenumber, ℓ is a positive integer and $m = -\ell, \dots, \ell$. The shear field, comprising γ_1 and γ_2 , can be written as components of a tensor, and expanded in terms of tensor spherical harmonics, as in Taylor (2001), or spin-spherical harmonics ${}_s Y_{\ell}^m$ as in Okamoto & Hu (2002). We will use the latter notation, generalised to 3D:

$$\gamma_1(\mathbf{r}) \pm i\gamma_2(\mathbf{r}) = \sqrt{\frac{2}{\pi}} \sum_{\ell m} \frac{1}{2} \sqrt{\frac{(\ell+2)!}{(\ell-2)!}} \int dk k^2 \gamma_{\ell m}(k) {}_{\pm 2} Y_{\ell}^m(\hat{\mathbf{n}}) j_{\ell}(kr). \quad (2)$$

In principle the coefficients $\gamma_{\ell m}(k)$ could depend on whether the + or - sign is taken, but they are the same, and are related to the transform of the lensing potential $\phi(\mathbf{r})$ by

$$\gamma_{\ell m}(k) = \frac{1}{2} \sqrt{\frac{(\ell+2)!}{(\ell-2)!}} \phi_{\ell m}(k) \quad (3)$$

(Taylor 2001). The lensing potential is related to the gravitational potential $\Phi(\mathbf{r})$ by a radial integral (e.g. Bartelmann & Schneider 2001)

$$\phi(\mathbf{r}) = \frac{2}{c^2} \int_0^r dr' \left[\frac{f_K(r) - f_K(r')}{f_K(r) f_K(r')} \right] \Phi(\mathbf{r}'). \quad (4)$$

$f_K(r) d\psi$ is the dimensionless transverse comoving separation for points separated by an angle $d\psi$. The Robertson-Walker metric may be written $ds^2 = c^2 dt^2 - R^2(t) [dr^2 + f_K^2(r) d\psi^2]$, and $f_K(r)$ takes the values $\sinh r$, r , $\sinh r$ for curvature values $k = 1, 0, -1$.

$\Phi(\mathbf{r})$ is related to the overdensity field $\delta(\mathbf{r}) \equiv \delta\rho(\mathbf{r})/\bar{\rho}$ by Poisson's equation

$$\nabla^2 \Phi = \frac{3\Omega_m H_0^2}{2a(t)} \delta, \quad (5)$$

where Ω_m is the matter density parameter, H_0 is the Hubble constant and $a(t) = 1/(1+z)$ is the scale factor. δ itself is not a homogeneous field, because it evolves with time, and hence with distance from the observer through the light travel time. In the linear regime, we can describe the growth by a universal growth rate $g(t)$ (see, for example Abazajian & Dodelson (2002) for quintessence models), so that $\delta = \delta^0 g(t)$, where $\delta^0(\mathbf{r})$ is the overdensity field, extrapolated using linear theory to the present day, and which is homogeneous. Thus $\Phi(\mathbf{r}) = \Phi^0 g(r)/a(r)$. Note that for an Einstein-de Sitter universe, $g(r)/a(r) = 1$, and that for the ‘concordance’ model of matter and vacuum density parameters $\Omega_m = 0.3$, $\Omega_v = 0.7$, $g(r)/a(r)$ declines from 1.28 at high redshift to unity today.

The transform of the lensing potential is therefore related to that of the present-day potential field by

$$\phi_{\ell m}(k) = \frac{1}{c^2} \int_0^\infty dk' k'^2 \eta_\ell(k, k') \Phi_{\ell m}^0(k') \quad (6)$$

where

$$\eta_\ell(k, k') \equiv \frac{4}{\pi} \int_0^\infty dr f_K(r) j_\ell(kr) \int_0^r dr' j_\ell(k'r') \left[\frac{f_K(r) - f_K(r')}{f_K(r')} \right] \frac{g(r')}{a(r')}. \quad (7)$$

These equations allow us to relate the coefficients of the shear field, $\gamma_{\ell m}(k)$ to the underlying linear, present-day overdensity field, $\delta_{\ell m}(k)$, since Poisson’s equation implies

$$\Phi_{\ell m}^0(k) = -\frac{3\Omega_m H_0^2}{2k^2} \delta_{\ell m}^0(k). \quad (8)$$

2.3 Discrete estimator

The data which we have to hand are estimates of the shear field at 3D positions in space, so it makes some sense to transform the data directly. The radial coordinate is generally not known accurately, but is typically given by a photometric redshift which has an error which may be $\sigma_z \sim 0.02 - 0.1$ or more. We denote this radial coordinate by s , and the true coordinate by r . They are related by a conditional probability, which we will take to be a gaussian

$$p(s|r) ds = \frac{1}{\sqrt{2\pi}\sigma_z} \exp\left[-\frac{(z_s - z_r)^2}{2\sigma_z^2}\right] dz_s \quad (9)$$

where $z_{r,s}$ are the redshifts associated with distance coordinates r and s . Note that σ_z can vary with z .

The estimate of the shear is obtained from the complex ellipticity (Bartelmann & Schneider 2001)

$$e = e^s + 2\gamma \quad (10)$$

where e^s is the intrinsic source ellipticity, whose mean is assumed to be zero, so $\hat{\gamma} = e/2$ is an unbiased, albeit noisy, estimate of the shear field. The shear estimates have covariance properties

$$\langle \hat{\gamma}_a \hat{\gamma}_b^* \rangle = \langle \gamma_a \gamma_b^* \rangle + \frac{1}{4} \langle e_a^s e_b^{s*} \rangle \quad (11)$$

for galaxies a and b . We denote the variance of e by σ_e^2 , typically $\lesssim 0.1$ (Hudson et al. 1998). The second term is non-

zero if galaxies are intrinsically aligned (see e.g. Heavens, Refregier & Heymans 2000). I ignore this term, as with photometric information, its effect can be removed by modifying the analysis to remove close pairs in three dimensions (Heymans & Heavens 2003; King & Schneider 2002). Thus we have noisy estimates $\hat{\gamma}$ of the shear field at imprecise positions with distances s given by photometric redshifts.

An obvious set of quantities to use for a harmonic description of the data is simply to do a discrete transform of the measurements which are to hand. We consider the following quantities:

$$\pm \hat{g}_{\ell m}(k) \equiv \sqrt{\frac{2}{\pi}} \sum_{\text{galaxies } \mathbf{g}} (\hat{\gamma}_{1g} \pm i\hat{\gamma}_{2g}) j_\ell(k s_g) \pm 2Y_\ell^m(\hat{\mathbf{n}}_g). \quad (12)$$

$\pm \hat{g}_{\ell m}(k)$ are estimates of the quantities

$$\pm g_{\ell m}(k) = \sqrt{\frac{2}{\pi}} \int d^3 \mathbf{s} n(\mathbf{s}) \gamma_\pm(\mathbf{r}) j_\ell(k s) \pm 2Y_\ell^m(\hat{\mathbf{n}}), \quad (13)$$

where $n(\mathbf{r})$ is the number density, and $\gamma_\pm \equiv \gamma_1 \pm i\gamma_2$. It is straightforward to include a non-uniform weighting of the galaxies if desired. This may improve the errors on parameter estimation, but is not explored in this paper.

Note that in this equation the shear field is evaluated at the true position \mathbf{r} , whereas the estimate (12) involves the distance s estimated from the photometric redshift. These are related by the conditional probability $p(s|r)$, leading to an average value of the expansion coefficients

$$\pm \bar{g}_{\ell m}(k) = \sqrt{\frac{2}{\pi}} \int d^3 \mathbf{s} \int dr p(s|r) n(\mathbf{s}) \gamma_\pm(\mathbf{r}) j_\ell(k s) \pm 2Y_\ell^m(\hat{\mathbf{n}}). \quad (14)$$

With the photometric redshift smoothing, $n(\mathbf{s})$ is heavily smoothed, so we can approximate it by the smoothed number density at \mathbf{r} , $n_s(\mathbf{r})$. For deep surveys, the angular clustering is small, so we can ignore clustering, and approximate this by the average number density, which normally separates into a radial part and an angular selection:

$$n_s(\mathbf{r}) = \bar{n}(r) M(\hat{\mathbf{n}}) \quad (15)$$

Normally $M = 0$ (unobserved sky) or $M = 1$ (in survey), although more complicated forms are possible, if some parts of the survey are partially sampled.

If we denote the spin-spherical harmonic transform of $n_s(\mathbf{r}) \gamma_\pm(\mathbf{r})$ by $\pm h_{\ell m}(k)$, i.e.

$$n_s(\mathbf{r}) \gamma_\pm(\mathbf{r}) = \sqrt{\frac{2}{\pi}} \sum_{\ell m} \int dk k^2 \pm h_{\ell m}(k) j_\ell(kr) \pm 2Y_\ell^m(\hat{\mathbf{n}}) \quad (16)$$

we find that (14) may be written

$$\begin{aligned} \pm \bar{g}_{\ell m}(k) &= \frac{2}{\pi} \int ds f_K^2(s) d\hat{\mathbf{n}} dr p(s|r) \\ &\sum_{\ell' m'} \int dk' k'^2 \pm h_{\ell' m'}(k') j_{\ell'}(k'r) j_\ell(k s) \\ &\pm 2Y_{\ell'}^{m'}(\hat{\mathbf{n}}) \pm 2Y_\ell^{m*}(\hat{\mathbf{n}}) M^2(\hat{\mathbf{n}}). \end{aligned} \quad (17)$$

It is convenient to define angular mixing matrices by

$$\pm W_{\ell \ell'}^{m m'} \equiv \int d\hat{\mathbf{n}} \pm 2Y_{\ell'}^{m'}(\hat{\mathbf{n}}) \pm 2Y_\ell^{m*}(\hat{\mathbf{n}}) M^2(\hat{\mathbf{n}}). \quad (18)$$

For all-sky coverage, $\pm W_{\ell\ell'}^{mm'} = \delta_{\ell\ell'}^K \delta_{mm'}^K$, where δ^K is the Kronecker delta symbol. Using W , we can simplify (17) to

$$\pm \bar{g}_{\ell m}(k) = \sum_{\ell'm'} \int dk' k'^2 \pm W_{\ell\ell'}^{mm'} Z_{\ell\ell'}(k, k') \pm h_{\ell'm'}(k') \quad (19)$$

where

$$Z_{\ell\ell'}(k, k') \equiv \frac{2}{\pi} \int ds f_K^2(s) dr p(s|r) j_{\ell'}(k'r) j_{\ell}(ks). \quad (20)$$

$\pm h_{\ell m}(k)$ may be calculated by direct substitution of the expansion of γ_{\pm} , yielding

$$\pm h_{\ell m}(k) = \int dk' k'^2 M_{\ell\ell'}(k, k') \pm \gamma_{\ell m}(k') \quad (21)$$

where

$$M_{\ell\ell'}(k, k') \equiv \frac{2}{\pi} \int dr f_K^2(r) j_{\ell'}(k'r) j_{\ell}(kr) \bar{n}(r). \quad (22)$$

(This equation is more general than necessary at this stage, with two indices ℓ and ℓ' , but $M_{\ell\ell'}$ will appear in its general form in the shot noise below). It is convenient to define a continuous form of the Einstein summation convention indicating integration over wavenumber:

$$A(k, k') B(k', k'') \equiv \int dk' k'^2 A(k, k') B(k', k''). \quad (23)$$

With this notation, we can write the shear expansion coefficients in terms of the present-day, linear density field coefficients as follows (from (18), (20), (7), (8) and (6)):

$$\begin{aligned} \pm \bar{g}_{\ell m}(k) &= -A \sum_{\ell'm'} \sqrt{\frac{(\ell'+2)!}{(\ell'-2)!}} \pm W_{\ell\ell'}^{mm'} Z_{\ell\ell'}(k, k') \\ &\quad M_{\ell\ell'}(k', \tilde{k}) \frac{\eta_{\ell'}(\tilde{k}, \tilde{k}')}{\tilde{k}'^2} \delta_{\ell'm'}^0(\tilde{k}') \end{aligned} \quad (24)$$

where $A \equiv 3\Omega_m H_0^2 / (4c^2)$. Note that the sums over ℓ' and m' are made explicitly.

For all-sky surveys, the average values of $\pm g_{\ell m}(k)$ are zero; information about cosmological parameters comes from their variance (or, more precisely, their covariance).

2.4 Covariance matrix of $\pm \bar{g}_{\ell m}(k)$

Since the present-day linear power spectrum is a homogeneous field, its covariance matrix is diagonal:

$$\langle \delta_{\ell m}^0(\tilde{k}) \delta_{\ell' m'}^{0*}(\tilde{k}') \rangle = \frac{P_{\delta}^0(k)}{k^2} \delta^D(k - k') \delta_{\ell\ell'}^K \delta_{mm'}^K \quad (25)$$

where δ^D is the Dirac delta function, and $P_{\delta}^0(k)$ is the present-day linear overdensity power spectrum.

The signal part of the covariance matrix is then

$$\begin{aligned} \langle \pm \bar{g}_{\ell m}(k) \pm \bar{g}_{\ell' m'}^*(k') \rangle &= A^2 \sum_{\tilde{\ell}\tilde{m}} \frac{(\tilde{\ell}+2)!}{(\tilde{\ell}-2)!} \pm W_{\ell\tilde{\ell}}^{m\tilde{m}} \pm W_{\ell'\tilde{\ell}'}^{m'\tilde{m}'} \\ &\quad Z_{\ell\tilde{\ell}}(k, k_1) Z_{\ell'\tilde{\ell}'}(k', k_2) M_{\tilde{\ell}\tilde{\ell}}(k_1, k_3) M_{\tilde{\ell}\tilde{\ell}'}(k_2, k_4) \\ &\quad \frac{\eta_{\tilde{\ell}}(k_3, k_5) \eta_{\tilde{\ell}'}(k_4, k_5)}{k_5^4} P_{\delta}^0(k_5). \end{aligned} \quad (26)$$

Note that if coverage is all-sky, the $\pm W$ matrices become delta functions and the covariance matrix simplifies consid-

erably to

$$\begin{aligned} \langle \pm \bar{g}_{\ell m}(k) \pm \bar{g}_{\ell' m'}^*(k') \rangle &= A^2 \frac{(\ell+2)!}{(\ell-2)!} Z_{\ell\ell}(k, k_1) Z_{\ell\ell}(k', k_2) \\ &\quad M_{\ell\ell}(k_1, k_3) M_{\ell\ell}(k_2, k_4) \frac{\eta_{\ell}(k_3, k_5) \eta_{\ell}(k_4, k_5)}{k_5^4} P_{\delta}^0(k_5) \delta_{\ell\ell'}^K \delta_{mm'}^K. \end{aligned} \quad (27)$$

2.5 Shot Noise

The shot noise can be computed via standard methods (e.g. Peebles 1980), by dividing the volume into cells i containing $n_i = 0$ or 1 galaxy.

$$\pm \hat{g}_{\ell m}(k) \equiv \sqrt{\frac{2}{\pi}} \sum_{\text{cells } i} n_i \hat{\gamma}_{\pm i} j_{\ell}(ks_i) \pm 2 Y_{\ell}^m(\hat{\mathbf{n}}_i). \quad (28)$$

so

$$\begin{aligned} \langle \pm \hat{g}_{\ell m}(k) \pm \hat{g}_{\ell' m'}^*(k') \rangle &= \frac{2}{\pi} \sum_{ij} \langle n_i n_j \hat{\gamma}_{\pm i} \hat{\gamma}_{\pm j}^* \rangle j_{\ell}(ks_i) \\ &\quad j_{\ell'}(ks_j) \pm 2 Y_{\ell}^{m*}(\hat{\mathbf{n}}_i) \pm 2 Y_{\ell'}^m(\hat{\mathbf{n}}_j). \end{aligned} \quad (29)$$

Assuming the shear field is uncorrelated with the presence or absence of a source galaxy, $\langle n_i n_j \hat{\gamma}_{\pm i} \hat{\gamma}_{\pm j}^* \rangle = \langle n_i n_j \rangle \langle \hat{\gamma}_{\pm i} \hat{\gamma}_{\pm j}^* \rangle$. Ignoring the small correlations in the smoothed density field,

$$\begin{aligned} \langle n_i n_j \rangle &= \langle n_i \rangle \quad (i = j) \\ &= \langle n_i \rangle \langle n_j \rangle \quad (i \neq j). \end{aligned} \quad (30)$$

The shot noise comes from the term $i = j$, for which

$$\langle |\hat{\gamma}_{\pm i}|^2 \rangle = \langle |\gamma_{\pm i}|^2 \rangle + \frac{\sigma_e^2}{4} \quad (31)$$

where the second term will dominate for weak lensing. Thus the shot noise may be written

$$\begin{aligned} \langle \pm \hat{g}_{\ell m}(k) \pm \hat{g}_{\ell' m'}^*(k') \rangle_{SN} &= \frac{\sigma_e^2}{2\pi} \int ds f_K^2(s) \bar{n}(s) \\ &\quad j_{\ell}(ks) j_{\ell'}(k's) \pm W_{\ell\ell'}^{mm'} \\ &= \frac{\sigma_e^2}{4} M_{\ell\ell'}(k, k') \pm W_{\ell\ell'}^{mm'}, \end{aligned} \quad (32)$$

using the definition (22).

3 ESTIMATION OF COSMOLOGICAL PARAMETERS

Various parts of this analysis are dependent on cosmological parameters: the matter power spectrum $P_{\delta}^0(k)$; the components of the metric $r(z)$ and $f_K[r(z)]$; the growth rate of perturbations $g(t)$. These parameters ($\{\theta_{\alpha}\}$) may be estimated from the data using likelihood methods. Assuming uniform priors for the parameters, the maximum a posteriori probability for the parameters is given by the maximum likelihood solution. For large-scale modes we use a gaussian likelihood

$$2 \ln L(\mathbf{g}|\{\theta_{\alpha}\}) = \text{constant} - \det(C) - \mathbf{g} \cdot C^{-1} \cdot \mathbf{g} \quad (33)$$

where $C = S + N$ is the covariance matrix, given by signal and noise terms (26) and (32). Note that the average values of \mathbf{g} (the set of $\pm \hat{g}_{\ell m}(k)$) is zero, so the information on the parameters comes from the dependence of the signal part of C . i.e. we adjust the parameters until the *covariance* of the model matches that of the data. This was the approach of

Heavens & Taylor (1995) and Ballinger, Heavens & Taylor (1995) in analysis of large-scale galaxy data.

Considering the vector \mathbf{g} as the data set has some advantages over more traditional methods such as the shear correlation function or the shear variance. The main one is that it is linear in the shear, so the covariance matrix is quadratic, and readily calculable. Quadratic estimators such as the shear correlation function have 4th order covariances, which can be cumbersome to calculate, even in gaussian, linear theory. We do, however, make an assumption that the covariance matrix is gaussian, and it requires numerical simulations to establish for which ranges of k and ℓ this is a good approximation.

3.1 Expected errors on cosmological parameters - the Fisher matrix

For a given experimental setup, the Fisher matrix gives the best errors to expect, provided that the likelihood surface near the peak is adequately approximated by a multivariate gaussian. We illustrate the effectiveness of a 3D analysis by analysing an all-sky survey with the following details, and compare some of the results with a 2D analysis of the same data. For smaller surveys, a reasonable approximation is to scale the errors by $f_{sky}^{-1/2}$, where f_{sky} is the fraction of sky observed. We assume that the average number density is $n(z) \propto z^2 \exp[-(z/z_*)^{1.5}]$ (cf (Baugh & Efstathiou 1993)), where $z_* = z_m/1.412$ and z_m is the median redshift of the survey, which we take to be 1. We assume a source density of 30 or 100 per square arcminute, errors on the ellipticity of 0.2 or 0.3, and a Λ CDM model with matter and vacuum density parameters of $\Omega_m = 0.3$, $\Omega_v = 0.7$.

The Fisher matrix is the expectation value of the second derivative of the $\ln L$ with respect to the parameters θ_α :

$$F_{\alpha\beta} = - \left\langle \frac{\partial^2 \ln L}{\partial \theta_\alpha \partial \theta_\beta} \right\rangle \quad (34)$$

and the marginal error on parameter θ_α is $\sqrt{(F^{-1})_{\alpha\alpha}}$ (Tegmark, Taylor & Heavens 1997). If the means of the data are fixed, the Fisher matrix can be calculated from the covariance matrix and its derivatives by (Tegmark, Taylor & Heavens 1997)

$$F_{\alpha\beta} = \frac{1}{2} \text{Trace} [C^{-1} C_{,\alpha} C^{-1} C_{,\beta}]. \quad (35)$$

For an all-sky survey, this simplifies, because modes with different ℓ and m are uncorrelated ($\pm W_{\ell\ell'}^{mm'} = \delta_{\ell\ell'}^K \delta_{mm'}^K$), so, defining C^ℓ as the covariance matrix for the modes with harmonic ℓ (and different k),

$$F_{\alpha\beta} = \frac{1}{2} \sum_{\ell} (2\ell + 1) \text{Trace} [(C^\ell)^{-1} C_{,\alpha}^\ell (C^\ell)^{-1} C_{,\beta}^\ell]. \quad (36)$$

For illustration, we have considered modes up to $\ell = 100$, and 100 k modes spaced equally between $k = 0.001$ and $0.1 h\text{Mpc}^{-1}$. These should be safely in the linear regime. The ℓ range can be extended, but at some point the linear approximation will break down, and the likelihood expression will deviate from a gaussian. The former may be tackled by using a nonlinear power spectrum, such as proposed by Peacock & Dodds (1996); the latter will need to be assessed by computer simulation.

(2D) Fractional Error on Power Spectrum

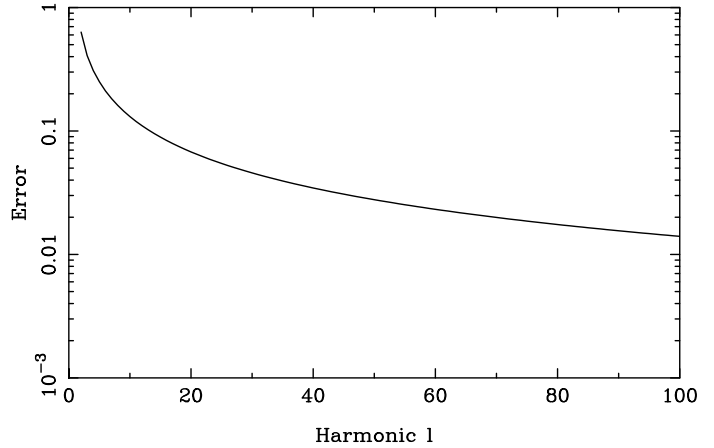


Figure 1. Fractional error on the amplitude of the linear matter density power spectrum, assuming all other parameters are known, from a 2D analysis of the survey, where individual source distance information is ignored. The figure shows the improvement as more harmonics are added up to $\ell = 100$. 100 radial wavenumber modes are considered between $k = 0.001$ and $0.1 h\text{Mpc}^{-1}$. Illustrated model is Λ CDM, with 100 source galaxies per square arcminute, and an ellipticity error of 0.2. Plot is cumulative, showing the reduction in error as more modes are included.

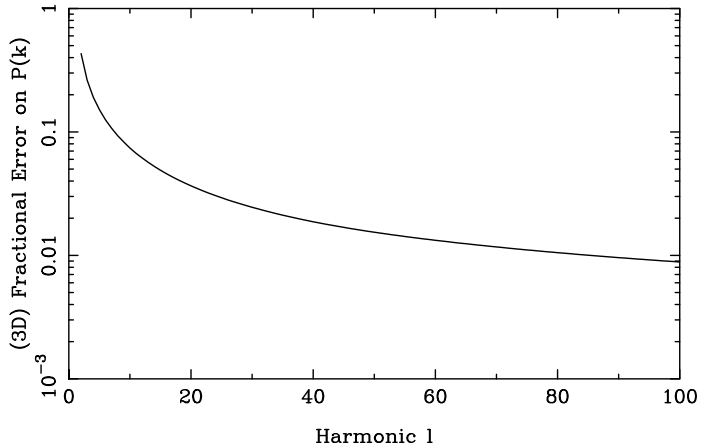


Figure 2. As Fig. 1, except that a 3D analysis is used, with photometric redshifts having an r.m.s. error of $\sigma_z = 0.02$.

3.2 Power spectrum amplitude

Fig. 1 and 2 show the improvement in the error on the fractional amplitude of the power spectrum as the number of ℓ modes is increased up to $\ell = 100$. For a 2D analysis, ignoring the distance information altogether, except for assuming $n(z)$ is known, the error is 1.4% for $\ell \leq 100$. Using the photometric redshift distance information improves this to 0.9%, assuming, perhaps optimistically, that the photometric redshift error is 0.02.

The improvement depends on the characteristics of the

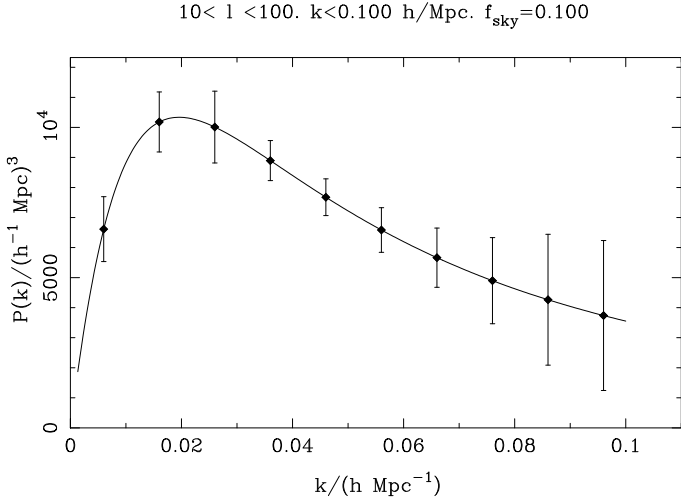


Figure 3. Band power estimates for a survey of 10% of the sky. The source number density assumed is 30 per square arcminute. The error bars are marginalised over the other bands. Note that the increase in the error at high k is a result of our truncating the analysis at $\ell = 100$. Increasing this would provide more information on the power spectrum at high k .

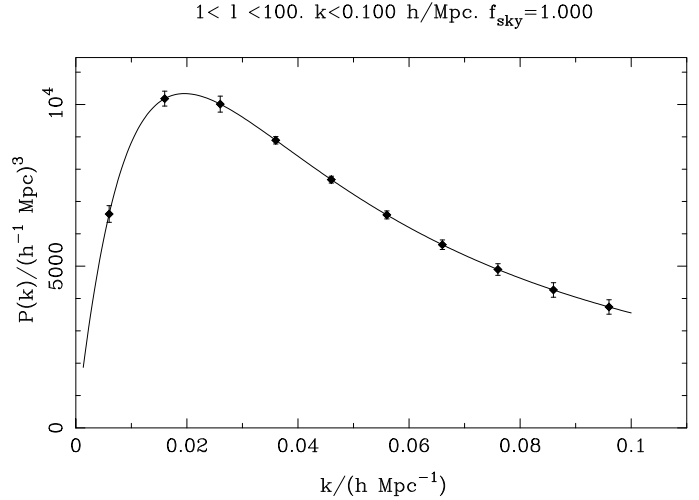


Figure 4. As Fig. 3, except survey is all-sky, intrinsic ellipticity dispersion is 0.2.

survey. Generally speaking, the better the lensing survey (higher number density of source galaxies, smaller ellipticity errors), the better the 3D analysis does in comparison with 2D, at least on the scales shown here. The reason is simply that the 3D modes are generally noisy, whereas the large-scale 2D modes are not. Improving the survey brings in more effective 3D modes which have good signal-to-noise. The effective number of good radial modes is investigated further in the Karhunen-Loeve analysis of section 4.

The Fisher analysis can be extended to calculate the errors arising if we estimate band powers from the 3D lensing data. The Fisher matrix is calculated as before, and its inverse used to estimate the errors on the band powers. Fig. 3 shows what may be achieved realistically for a survey of 10% of the sky, with a median redshift of 1. Fig. 4 is for an optimistic all-sky survey and optimistic errors.

3.3 Vacuum Energy equation of state

The most exciting prospect of 3D lensing analysis is to measure the equation of state parameter, w , of the vacuum energy, defined in terms of its pressure and energy density by $p_v = w\rho_v c^2$. The equation of state of the vacuum energy influences the lensing signal in two ways. Firstly, the growth rate of perturbations differs; secondly, the distance-redshift relation is changed. I use the growth rate from Abazajian & Dodelson (2002) for quintessence models, and the distance-redshift relation is obtained from the integral

$$r = \int_0^z \frac{dz'}{H(z')} \quad (37)$$

where for flat models $H(z) = H_0[(1 - \Omega_v)(1 + z)^3 + \Omega_v(1 + z)^{3(1+w)}]^{-1/2}$ is the Hubble parameter in terms of the present day Hubble parameter H_0 , and Ω_v is the present vacuum energy density parameter.

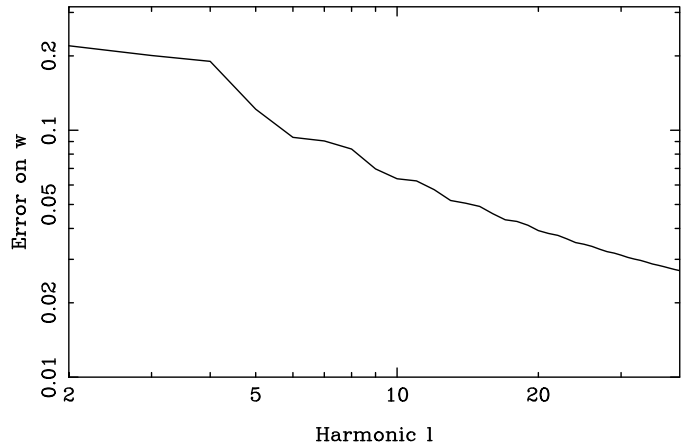


Figure 5. The expected error on w for a survey covering 10% of the sky to a median redshift of 1, with 100 galaxies per square arcminute, and a photometric redshift error of 0.02, and an ellipticity error of 0.3. The plot is cumulative to harmonic ℓ . In practice for partial sky coverage the low- ℓ modes will not be accessible, but this will hardly change the results.

The sensitivity to w can then be calculated by computing the Fisher matrix (scalar), equation (36), where the derivative of the covariance matrix is obtained by finite differencing. Note that this figure is optimistic in the sense that the errors it produces assume that all other parameters are known, not altogether unrealistic with the success of microwave background experiments. On the other hand, $\ell = 40$ is a reasonably large scale ($\sim 5^\circ$), and there is more information available at higher ℓ , so 1% accuracy is probably achievable.

4 KARHUNEN-LOÈVE ANALYSIS

For all-sky surveys, the coupling of modes is only between those of the same ℓ and m , so the data analysis task is relatively straightforward, as each set of ℓ and m can be analysed separately. For partial sky coverage, the modes get mixed, and the covariance matrix gets very large. Data compression techniques such as signal-to-noise eigenmodes, Karhunen-Loève (KL) transformations and the like can be extremely valuable in reducing the size of the data set whilst having minimal impact on the error bars on the recovered parameters. These have been used extensively in studies of large-scale structure and the microwave background (refs).

The procedure is detailed, for example, in Tegmark, Taylor & Heavens (1997), and involves finding linear combinations of the data which are uncorrelated and which are ordered in decreasing order of the information which they yield on a parameter. This involves solving a generalised eigenvalue problem

$$C_{,\alpha} \mathbf{b} = \lambda C \mathbf{b} \quad (38)$$

where θ_{α} is the parameter of interest. The eigenvalues λ quantify how much information each linear combination $\mathbf{b} \cdot \mathbf{x}$ of the data \mathbf{x} provides, and very often this declines sharply with mode number, so the dataset can be compressed substantially without significantly increasing the error bar. Here, we calculate the KL modes appropriate for the (natural log of the) amplitude of the matter power spectrum, in which case $C_{,\alpha} = S$. The problem then is equivalent to finding signal-to-noise eigenmodes, e.g. Vogelely & Szalay (1996). Fig. 6 shows the signal-to-noise of the best modes for each of the low-order multipoles. We see that there are roughly 4 useful modes with $S/N > 1$. In other words, there is some extra information on the power spectrum coming from the 3D information, but the added accuracy is limited - the analysis had 100 radial wavenumbers. This is broadly in agreement with the findings of Hu (1999), who found that division of the source population into two, on the basis of redshift, improved the error bars on the power spectrum by a factor of 2, but that further division yielded little extra accuracy.

It is quite instructive to look at the KL modes themselves. Fig. 7 shows the best radial KL modes corresponding with the low-order angular multipoles. We see several interesting features. Firstly, the best two modes between them weight the data reasonably uniformly, apart from a drop-off at small distances. This latter behaviour is expected, as the lensing is ineffective at low redshift. The near-uniform weighting suggests that a 2D survey is not too bad - it corresponds to equal weighting, and matches quite well the single best mode of the KL analysis. For other parameters, this may not hold.

The other interesting and encouraging feature of these graphs is that the good modes are long-wavelength, suggesting that having precise photometric redshifts is not necessary to get most of the information present in the data.

5 CONCLUSIONS

In this paper, I have shown how photometric redshifts may be used to perform a full 3D statistical analysis of the shear

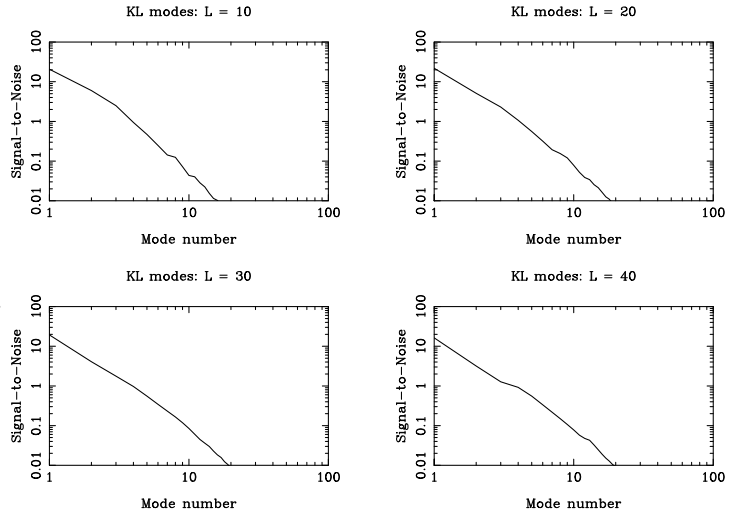


Figure 6. Signal-to-noise eigenmode analysis of the sample survey, for a few of the low-order angular modes. We see that there are about 4 useful linear combinations of the radial k modes.

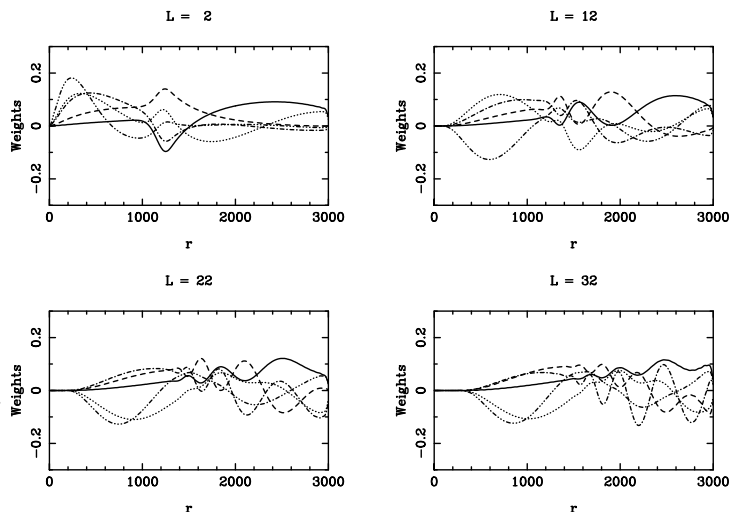


Figure 7. KL modes corresponding to the low-order multipoles. In each case the best mode is solid, and the dashed, dot-dashed, dotted and the dash-dot-dot-dotted lines show the next 4 modes in decreasing order of usefulness. Note that a) the best couple of modes largely ignore the distance information, as in a 2D survey, and b) the best modes are long-wavelength - accurate photometric redshifts may not be required.

field in weak lensing surveys. With photometric redshifts, one has an estimate of the lensing shear field at the (estimated) positions of the source galaxies in three dimensions, and there is no particular reason to throw this away by ignoring the distance information or by dividing the source galaxy population into shells.

Determining the properties of the vacuum energy, which makes up $\sim 70\%$ of the energy density of the Universe, is one of the most important current goals in cosmology. These properties are not easy to determine accurately using the microwave background alone, which has been so successful in recent years in pinning down other cosmological parameters

(e.g. Spergel et al. 2003). I show in this paper that 3D lensing analysis offers the possibility of high-precision measurement of the equation of state parameter w (defined such that the vacuum has $p_v = w\rho_v c^2$), with an accuracy of 1% being a realistic possibility. With higher angular resolution than investigated here, the prospects of getting good constraints on $w(z)$ are good, and the possibilities of testing specific predictions of $w(z)$ from models of the vacuum energy are excellent. For other parameters, such as the amplitude of the matter power spectrum, 3D information reduces the error bars by modest factors. A signal-to-noise eigenmode analysis suggests that there are a few radial modes which are useful for this purpose. This analysis also shows that the high signal-to-noise modes have little high-frequency structure, so even modestly accurate photometric redshifts can be useful.

In addition to the advantages in reducing the statistical error on parameters, photometric redshifts also allow elimination of a number of possible systematic effects, arising from physical processes, which could otherwise eventually limit the accuracy of weak lensing studies. For cosmic shear measurements in particular, the dominant physical systematic may be the intrinsic alignment of galaxies arising from tidal forces during and after formation (Heavens, Refregier & Heymans 2000; Croft & Metzler 2000; Crittenden et al. 2001; Catelan, Kamionkowski & Blandford 2001; Mackey, White & Kamionkowski 2002; Jing 2002). Heymans & Heavens (2003) and King & Schneider (2002) showed how photometric redshifts can be used to remove nearby pairs from the analysis and essentially remove the intrinsic alignment contamination to high accuracy. The advantages in reduced statistical and systematic errors make a compelling case for obtaining photometric redshifts for cosmic shear surveys.

6 ACKNOWLEDGMENTS

I would like to thank Andy Taylor, Meghan Gray, David Bacon and Catherine Heymans for useful discussions.

REFERENCES

- Abazajian K. N., Dodelson S., 2002. astro-ph, 0212216.
 Bacon D. J., Taylor A. N., 2002. astro-ph, 0212266.
 Bacon D. J., Refregier A. R., Ellis R. S., 2000. MNRAS, 318, 625.
 Ballinger W. E., Heavens A. F., Taylor A. N., 1995. MNRAS, 276, 59P.
 Barber A. J., Thomas P. A., Couchman H. M. P., Fluke C. J., 2000. MNRAS, 319, 267.
 Bartelmann M., Schneider P., 2001. Physics Reports, 340, 291.
 Baugh C. M., Efstathiou G., 1993. MNRAS, 265, 145.
 Bond J. R., 1995. Phys. Rev. Lett., 74, 4369.
 Broadhurst T. J., Taylor A. N., Peacock J. A., 1995. ApJ, 438, 49.
 Brown M., Taylor A., Bacon D. J., Gray M. E., Meisenheimer K., Dye S., Wolf C., 2002a. astro-ph, 0210213.
 Brown M., Taylor A., Hambly N., Dye S., 2002b. MNRAS, 333, 501.
 Catelan P., Kamionkowski M., Blandford R. D., 2001. MNRAS, 320, L7.
 Couchman H. M. P., Barber A. J., Thomas P. A., 1999. MNRAS, 308, 180.
 Crittenden R., Natarajan P., Pen U.-L., Theuns T., 2001. ApJ, 559, 552.
 Croft R. A. C., Metzler C. A., 2000. apj, 545, 561.
 Hamana et al. T., 2002. astro-ph, 0210450.
 Heavens A. F., Taylor A. N., 1995. MNRAS, 275, 483.
 Heavens A. F., Refregier A., Heymans C. E. C., 2000. MNRAS, 319, 649.
 Heymans C. E. C., Heavens A. F., 2003. MNRAS, 339, 711.
 Hu W., Keeton C. R., 2002. Phys. Rev. D, 66, 63506.
 Hu W., 1999. ApJ(Lett), 522, L21.
 Hudson M. J., Gwyn S. D. J., Dahle H., Kaiser N., 1998. ApJ, 503, 531.
 Jarvis M., Bernstein G. M., Fischer P., Smith D., Jain B., Tyson J. A., Wittman D., 2003. AJ, 125, 1014.
 Jing Y. P., 2002. MNRAS, 335, L89.
 King L., Schneider P., 2002. A& A, 396, 411.
 Mackey J., White M., Kamionkowski M., 2002. MNRAS, 332, 788.
 Okamoto T., Hu W., 2002. Phys. Rev. D, 66, 63008.
 Peacock J. A., Dodds S. J., 1996. MNRAS, 280, 19P.
 Peebles P. J. E., 1980. *The Large Scale Structure of the Universe*, Princeton University Press.
 Taylor A. N., Bacon D. J., Gray M. E., Meisenheimer K., Dye S., 2003. MNRAS, in preparation.
 Spergel D. N. et al., 2003. astro-ph, 0302209.
 Taylor A. N., 2001. astro-ph, 0111605.
 Tegmark M., Taylor A., Heavens A., 1997. ApJ, 480, 22.
 Van Waerbeke L., Mellier Y., Erben T., Cuillandre J. C., Bernardeau F., Maoli R., Bertin E., Mc Cracken H. J., Le Fèvre O., Fort B., Dantel-Fort M., Jain B., Schneider P., 2000. A& A, 358, 30.
 Verde L. et al., 2002. MNRAS, 335, 432.
 Vogeley M. S., Szalay A. S., 1996. ApJ, 465, 34+.
 Wittman D., Tyson J. A., Margoniner V. E., Cohen J. G., Dell'Antonio I. P., 2001. ApJ(Lett), 557, L89.
 Wittman D., Margoniner V. E., Tyson J. A., Cohen J. G., Dell'Antonio I. P., 2002. astro-ph, 0210120.